J Solid State Electrochem (2016) 20:2491–2501
DOI 10.1007/s10008-015-3078-2

ORIGINAL PAPER

Voltammetric sensor based on magnetic particles modified composite electrode for determination of triamterene in biological sample

Felipe Fantinato Hudari[1] · **Bianca Ferreira da Silva**[1] · **Maria Isabel Pividori**[2] · **Maria Valnice Boldrin Zanoni**[1]

Received: 1 October 2015 / Revised: 3 November 2015 / Accepted: 6 November 2015 / Published online: 17 November 2015

Abstract Some diuretic substances are controlled and monitored by the World Anti-Doping Agency as prohibited substances for use by athletes, such as triamterene (TRT). Thus, this work describes a voltammetric method based on graphite-epoxy composite electrode modified by tosyl-functionalized magnetic particles (GECE/MPs-To) for determination of TRT diuretic in urine sample. The TRT presented an oxidation peak at +1.24 V at GECE/MPs-To with irreversible behavior. Controlled potential electrolysis of the TRT at +1.26 V indicated the two electrons are transferred during amine group oxidation and the main product was identified by LC-MS/MS. The anodic peak current is 25 % higher at the modified electrode, suggesting that TRT is adsorbed on the magnetic particles. Using optimized conditions by using multivariate optimization of the parameters inherent of the square wave voltammetry, a calibration curve was constructed with a linear relationship for TRT from 0.500 to 99.8 μmol L^{-1}. The limits of detection and quantification were 1.47 and 4.91×10^{-7} mol L^{-1}, respectively. The proposed method was applied to urine sample and validated by LC-MS/MS technique where the values found and compared between the two techniques showed no significant difference at 95 % confidence.

Keywords Magnetic particles · Triamterene · Diuretic · Graphite-epoxy composite electrode · Voltammetric sensor · Multivariate optimization

✉ Felipe Fantinato Hudari
felipe_fhudari@hotmail.com

[1] Departamento de Química, UNESP, Universidade Estadual Paulista Júlio Mesquita Filho, Instituto de Química de Araraquara, Rua Francisco Degni, 55, Bairro Quitandinha,, 14800-900 Araraquara, SP, Brazil

[2] Departamento de Química, Grupo de Sensor e Biosensor, Universidade Autônoma de Barcelona, Bellaterra, 08193 Barcelona, Spain

Introduction

The magnetic particles (MPs) have been overexploited as drug carrier materials, cancer therapy, hyperthermia, magnetic separation, magnetic resonance, catalysis, sensors, and biosensors [1–14]. As an example of the use of the MPs as biosensors, in the work of Lermo et al., the researchers proposed a biosensor based on the immobilization of the protein conjugate BSA-folic acid in magnetic beads functionalized with tosyl group and subsequent preconcentration using a composite electrode for the determination of folic acid in vitamin-fortified milk sample. Thus, through analysis in 0.01 mol L^{-1} phosphate buffer solution (pH 7.5), the detection limit and the linear relationship were 6 nmol L^{-1} and 18.1 to 323.9 nmol L^{-1} in phosphate buffer solution and 13.1 nmol L^{-1} and 21.1 to 129.3 nmol L^{-1} in milk reference solution, respectively [15]. Mani and co-authors also demonstrated that glassy carbon electrode modified with iron nanoparticles decorated with nanocomposites of graphene/multiwalled carbon nanotubes can successfully be used for determining nitrite in water samples. Under optimized conditions, the amperometric detection of nitrite occurs at +0.77 V in 0.05 mol L^{-1} phosphate buffer solution (pH 5.0) reaching detection limit of 75.6 nmol L^{-1} [16].

In general, the most promising MPs are iron oxide particles that can be found in various types such as magnetite (Fe_3O_4), maghemite (γ-Fe_2O_3), and hematite (α-Fe_2O_3) [17, 18]. Among these, magnetite is most extensively studied due to their superparamagnetic behavior at room temperature. In addition to this characteristic, Fe_3O_4 is suitable for its

incorporation into biological areas, because it has no toxicity, presents high biocompatibility, and is easy to be obtained such as: sol-gel, co-precipitation, hydrolysis, and thermal decomposition [19–22].

The interest in magnetite particles in electrochemical area is based on their easy use when applied to the modification of electrodes, high adsorption of analyte, and a large surface area, increasing the pre-concentration of the analyte of interest obtaining, thus, low levels of detection as described by several authors [23–25].

Bagheri et al. [24] have reported the use of magnetite/carbon nanotube paste electrode for voltammetric determination of haloperidol. Using optimized conditions of 0.10 mol L^{-1} Britton–Robinson (B–R) buffer solution (pH 7.5), the authors reached detection limits of 7.02×10^{-10} and 1.33×10^{-10} mol L^{-1} for differential pulse voltammetry (DPV) and square wave voltammetry (SWV), respectively. Yin et al. [25] have shown that a voltammetric sensor based on graphene, chitosan, and Fe_3O_4 nanoparticles modified glassy carbon electrode for the determination of guanine in urine sample. Linear calibration curves were obtained from 2.00×10^{-6} to 3.50×10^{-4} mol L^{-1} of guanine in 0.1 mol L^{-1} phosphate buffer solution (pH 7.0).

Triamterene (Fig. 1) is a diuretic substance prohibited by the World Anti-Doping Agency (WADA) for athletes. Although it is widely used in hypertension treatments, combat of heart failure, cirrhosis, pulmonary disease, among others [26, 27], they are also used in order to increase the urinary flow while consequently decreasing the chance of detecting other illegal substances or even reducing the body weight of athletes [28]. By taking into account that competent toxicological trials in clinical and forensic toxicology usually require highly sensitive and selective analytical methods, the use of voltammetric sensor based on MPs could represent a great advantage.

The main analytical methods reported in literature for its determination are high-performance liquid chromatography [29], cloud point extraction combined with spectrofluorimetry [30], fluorescence spectroscopy [31], gas chromatography mass spectrometry [32], and electrochemical techniques [33, 34]. Nevertheless, there are few studies reporting the determination and quantification of this diuretic in biological samples such as blood or urine [35]. In the work of Ensafi and Hajian [34], the authors proposed an electroanalytical method using hanging mercury drop electrode for the determination of the triamterene and losartan in urine sample. Through analysis in 0.1 mol L^{-1} B–R buffer solution (pH 3.0) using cathodic adsorptive stripping square wave voltammetric, a limit of detection of 9.70 and 0.300 nmol L^{-1} was found for losartan and triamterene, respectively. Therefore, the analytes were not found in the urine sample.

Thus, the present work aims to develop a sensor based on the tosyl group-functionalized magnetic particles modifying graphite-epoxy composite electrode for the determination of the diuretic assigned as triamterene (Fig. 1) in the urine sample. For this, the electrochemical oxidation mechanism and also the use of 2^3 factorial design, Doehlert matrix, and multi-response methodology to improve the knowledge about the oxidation process and also to improve the detection of this pharmaceutical compound in the biological fluid were studied.

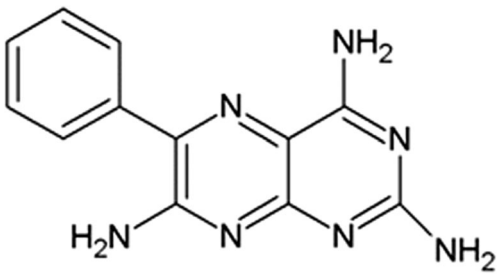

Fig. 1 Chemical structure of triamterene

Experimental

Reagents and equipments

All chemicals used in this work were of analytical grade, and the solutions were prepared using ultra-pure water (Milli-Q® system, Millipore). Triamterene (purity ≥99.9 %) and dimethylsulfoxide were obtained from Sigma-Aldrich. Boric acid, phosphate acid, acetic acid, ammonium chloride, and potassium chloride were from Merck. Sodium hydroxide was obtained from Synth. Magnetic particles functionalized with tosyl group were obtained from Life Technologies®. Standard solution of 0.01 mol L^{-1} of triamterene was prepared by dissolution in dimethylsulfoxide (DMSO), which was diluted afterwards in Britton–Robinson buffer (B–R) 0.10 mol L^{-1} used as supporting electrolyte. The B–R buffer was prepared by mixing appropriated amounts of 0.10 mol L^{-1} sodium hydroxide to orthophosphoric acid, acetic acid, and boric acid (0.10 mol L^{-1} in each) solution. Measurements of pH were carried out in a TECNOPON mPA 210 pH-meter. The electrochemical experiments were carried out in a potentiostat/galvanostat Autolab PGSTAT302N controlled by the NOVA software, using three electrodes.

Graphite-epoxy composite electrode modified by tosyl-functionalized magnetic particles

The composite electrode was constructed by using a graphite powder and epoxy resin prepared according to a method described in literature [36, 37]. Graphite powder and epoxy resin (1:4) were mixed, and after forming a paste, a thin layer of the

mixture was placed to a depth of 3 mm in a cylindrical PVC bat (6 mm i.d.) with an electrical contact to promote contact. A cylindrical magnet (3-mm diameter) was then placed into the center of this electrode, and the body of the electrode was filled with the paste. After filling, the electrode was tightly packed and maintained at rest at 40 °C for 1 week to obtain a rigid composite. After electrode preparation, a suspension of 30 mg mL^{-1} of magnetic particles functionalized with tosyl groups (MPs-To) was diluted in aqueous medium to generate a final solution of 1 mg mL^{-1}. Next, 30 μL of the suspension MPs-To was added to the surface of the composite electrode, which was used after evaporation of the solvent for 2 h at room temperature.

Electrochemical analysis

All electrochemical measurements were conducted in an electrochemical cell of 10.0 mL in a conventional system three-electrode containing the work (composite electrode with and without modification by MPs-To), auxiliary (platinum wire), and reference (Ag|AgCl; KCl, 3 mol L^{-1}) electrodes. After modification of the composite electrode with MPs-To, the electrode was subjected to several electrochemical cycling from 0.8 to 1.4 V in 0.10 mol L^{-1} B–R buffer solution (pH 6.0).

Controlled potential electrolysis of triamterene (TRT) diuretic was carried out in an electrochemical cell of 75.0 mL containing the work (platinum mesh), auxiliary (Ti/Ru sheet of 25 cm^2), and reference (Ag|AgCl; KCl, 3 mol L^{-1}) electrodes in 0.10 mol L^{-1} B–R buffer solution (pH 6.0). For these curves of current vs time, a fixed potential of 1.26 V was applied, when the flat current was obtained.

LC-MS/MS analysis

Analysis of LC-MS/MS for TRT diuretic and generated electrolyzed products after 3 h at +1.26 V was performed in a high-performance liquid chromatography of 1200 Agilent Technologies coupled to a Mass Spectrometer 3200 QTRAP (Quadrupole Linear Ion Trap LC-ESI-MS/MS) equipped with a Phenomenex Kinetex PFP column (150×4.6 mm; 5 μm). The analysis conditions were based on Murray and Danaceau with some modifications [38]. Sample elution was performed using a gradient mode of a mixture of ultra-pure water containing 0.10 % formic acid (A) and methanol (B). For the analysis of the TRT degradation, the following gradient programming was used: 0–2 min 5 % B, 2–12 min 5–100 % B, 12–13 min 100 % B, 13–14 min 100–5 % B, and 14–20 min 5 % B, using the flow rate of 1 mL min^{-1} and sample injection volume of 20 μL.

The ion source was operated in an electrospray positive mode at 600 °C in the following conditions of ionization: ion spray voltage (IS)=5500 V; curtain gas (CUR)=20 psi; nebulizer gas_1=50 psi; nebulizer gas_2=50 psi; declustering potential (DP), 31 V; and entrance potential (EP), 10 V.

The experiments for the investigation of the oxidation products were performed by software LightSight® (SCIEX), where a series of pre-programmed reactions were investigated based on the fragment ion spectrum of the TRT standard. All the experiments were tested by enhanced mass scan (EMS), and selected reaction monitoring (SRM) with simultaneous acquisition of fragment ion experiments was performed.

Urine samples

The method was applied in the analysis of TRT diuretic in human urine sample using the following procedure: 10 mL of urine sample was collected from a healthy person who volunteered, which was spike to 4.93 μmol L^{-1} of TRT. Two milliliters of this sample was diluted in 8 mL of 0.10 mol L^{-1} B–R buffer solution (pH 6.0) in the electrochemical cell and analyzed without any pretreatment of the sample.

The validation of the proposed method was obtained using analyzes of TRT in the same sample by using LC-MS/MS, after previous dilution of five times and sample cleaning. The sample pretreatment was performed using 2 mL of the urine spiked to TRT and submitted to an extraction step in a Phenomenex Strata-X 33u cartridge (200 mg, 3 mL), previously conditioned with methanol (3 mL) and Milli-Q water (3 mL). After sample loading, the sorbent was washed with 2 mL of Milli-Q water. After drying for 1 min under nitrogen gas flow, the analyte was eluted with 2 mL methanol and then an aliquot (150 μL of sample+150 μL of Milli-Q water) was inserted in vials for analysis in the LC-MS/MS.

The LC-MS/MS methodology was performed using a selected reaction monitoring (SRM) experiment, where three transitions of the compound were monitored from the standard optimization by direct infusion at the concentration of 0.10 ppm to 10 μL min^{-1}. The parameters of SRM were monitored (Table 1)

Ionizations in a positive mode condition were the same as described in "LC-MS/MS analysis." For the LC analysis, the same mobile phase was used, however, with a different gradient elution: 0–2 min 30 % B, 2–4 min 100 % B, 4–5 min 100 % B, 5–6 min 100–70 % B, and 6–10 min 70 % B. The

Table 1 Parameters of SRM

Precursor ion (Q1)	Fragment ion (Q3)	Collision energy (V) (CE)	Cell exit potential (V) (CXP)
254>	237	23	4
254>	104	51	4
254>	141	55	4

flow rate was 1 mL min^{-1} and sample injection volume of 20 μL.

Results and discussion

Electrochemical oxidation of TRT

Cyclic voltammograms obtained for 100 μmol L^{-1} triamterene in 0.10 mol L^{-1} B–R buffer, pH 4.0, at the composite electrode before (curve a) and after (curve b) modification with magnetic particles functionalized with tosyl group are shown in Fig. 2(I). An anodic peak is observed at 1.30 V (without) and at 1.24 V (with modification), and no cathodic peak is observed at reverse scan. The anodic peak increased 25 % at the modified electrode, suggesting that the TRT is preconcentrated on the electrode surface. This behavior can be assigned due to the hydrogen bonds between the hydrogen of the amine of the molecule of TRT with the sulfone group present in the molecule of the tosyl group.

The effect of the successive cycles on the voltammograms recorded for TRT using graphite-epoxy composite electrode modified by tosyl-functionalized magnetic particles (GECE/MPs-To) is shown in Fig. 2(II). It is observed that that anodic peak decreases dramatically after the first scan, indicating that the oxidation product of the TRT also adsorbs on the electrode surface. The spontaneous adsorption is very fast, since there was no current increased when accumulation time (0–5 min) was studied. However, to minimize problems and surface renewal, prior to analysis, the solution was stirred for 20 s to remove the oxidized species, when the peak intensity is completely recovered.

The scan rate effect of oxidation of TRT

The effect of the scan rate ( ) in the anodic peak (I_{ap}) intensity was investigated from 5.00 to 200 mV s^{-1} for 100 μmol L^{-1} of TRT in 0.100 mol L^{-1} B–R buffer solution. The I_{ap} increased according to a linear relationship with equation $I_{ap}=(5.54\pm0.18)\times10^{-5}+(10.0\pm1.7)\times10^{-7}$ ($R^2=0.990$). This behavior is an indicative that the charge transfer is controlled by adsorptive process [39].

The active area of the modified electrode was calculated by the Randles–Sevcik equation ($I_{ap}=2.69\times10^5 n^{3/2}AD_0^{1/2}C_0v^{1/2}$) [39], where, I_{ap} is the intensity of the anodic peak (μA), n is number of electron, A is the active area of the electrode (cm^2), D_0 is the diffusion coefficient ($cm^2\ s^{-1}$), $v^{1/2}$ is the square root of the scan rate (V s^{-1}), and C_0 is the analyte concentration (mol cm^{-3}). The active area for the GECE/MPs-To was estimated as 0.167 cm^2, taking cyclic voltammograms recorded for 1.00 mmol L^{-1} potassium hexacyanoferrate (III) as model compound in 1.00 mol L^{-1} KCl solution (diffusion coefficient=7.60×10^{-6} $cm^2\ s^{-1}$) [39]. The diffusion coefficient for TRT was 3.50×10^{-6} $cm^2\ s^{-1}$, obtained from Randles–Sevcik (for irreversible process $I_{ap}=2.99\times10^5\alpha^{1/2}n^{3/2}AD_0^{1/2}C_0v^{1/2}$) equation [39] and the respective voltammograms for 100 μmol L^{-1} of TRT between 5 and 100 mV s^{-1} in 0.100 mol L^{-1} B–R buffer (pH 6.0).

In order to find out the surface excess of diuretic on GECE/MPs-To, analysis for 100 μmol L^{-1} of the analyte was carried in the range of scan rate of 20 to 75 mV s^{-1}. From equation $I_{ap}=\frac{\alpha F^2AvT}{2.718RT}$ [39],where , A, and I_{ap} are the scan rate, the electrode active area of electrode, and the current peak, respectively, and other symbols have their usual meanings, the concentration of TRT at the surface of the GECE/MPs-To is 3.18×10^{-10} mol L^{-1}. The electron transfer coefficient (α) can be calculated from $n\alpha=\frac{47.7\ mV}{(E_{ap}-E_{1/2})}$ [39] taken from the cyclic voltammograms that indicate value of $n\alpha$=1.68. Knowing that the value of n is 2 (sections "The effect of pH on oxidation of TR" and "Controlled potential electrolysis of the TRT"), the value of α is 0.84.

The effect of pH on oxidation of TRT

The effect of pH on oxidation of 100 μmol L^{-1} of TRT in 0.10 mol L^{-1} B–R was evaluated from pH 4 to 9. Higher pH value promotes the diuretic deprotonation resulting in the

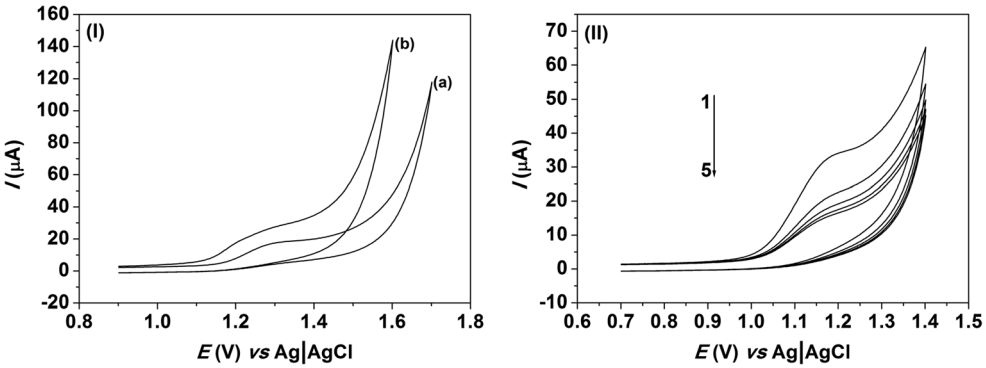

Fig. 2 Cyclic voltammograms for 100 μmol L^{-1} of TRT in 0.10 mol L^{-1} B–R buffer solution (pH 4.0) using GECE (*a*) and GECE/MPs-To (*b*) (*I*) and cyclic voltammograms successive for 100 μmol L^{-1} of TRT in 0.10 mol L^{-1} B–R buffer solution (pH 6.0) using GECE/MPs-To (*II*). Scan rate, 75 mV s^{-1}

decreased of hydrogen bonds between the analyte and the MPs-To. Higher current intensity was found at pH 6 coupled to better peak resolution, which was chosen at further studies. In addition, a shifting of anodic peak potential (E_{ap}) to more negative potentials was observed, whose slope is −59 mV/αn, suggesting that the ratio of e^-/H^+ for oxidation of TRT is around 1 [39]. In agreement with the predict for irreversible process with analyte adsorption [40], $E_{ap} = E^0 - \left(\frac{RT}{\alpha nT}\right)\ln\left(\frac{RTk_s}{\alpha nF}\right) + \left(\frac{RT}{\alpha nF}\right)$ ln v, where α is the coefficient of electron transfer, k_s the heterogeneous electron transfer rate constant, n the number of electrons transferred, the scan rate, and E^0 is the formal redox potential. Thus, the term αn can be obtained by the slope of the relationship between E_{ap} vs ln . Substituting the values of E_{ap} vs ln (0.0157), R (8.314), T (298), and F (96,480), the αn is equal to 1.63. So, knowing that the value of α is equal to 0.84, the number of electrons that participate in the oxidation process of TRT is 1.95 (n=2), confirming the value found in section "Controlled potential electrolysis of the TRT." Thus, as the proportion of e^-/H^+ is the same, the amount of protons that participate in reaction is equal to 2. In order to obtain more details about the electrochemical oxidation of TRT, further studies were carried out using controlled potential electrolysis.

Controlled potential electrolysis of the TRT

The oxidations were carried out for 100 μmol L^{-1} of the TRT in 0.10 mol L^{-1} B–R buffer solution (pH 6.0) using a Pt electrode. The electrolysis was performed at a potential more positive than the oxidation peak recorded on this electrode (+ 1.26 V vs Ag/AgCl) during 3 h. The current was recorded as a function of time, and the number of electrons (n) consumed in the total oxidation was determined. The current decays exponentially with time and the n values obtained are around two electrons (valor real±0.220 with three repetitions).

At the end of the electrolysis, the products at the anode were examined by LC-MS/MS in agreement with the procedure described in experimental section. The total ion chromatogram (TIC) of the control sample (TRT solution before electrolysis) showed a peak at 7.9 min (Fig. 3a) with m/z 254 corresponding to TRT (MW. 253 Da, $[M+H]^+$) (Fig. 3b). The same analysis was performed with the electrolysis sample and as observed at Fig. 3d, the TRT was still present (m/z 254 at retention time of 8.0 min), and another peak was detected at 8.9 min with m/z 252 ($[M+H]^+$) (Fig. 3e). The mass difference of 2.0 Da observed confirmed the oxidation product of TRT. MS^2 experiments were also performed for both compounds. The TRT fragment ion spectra (Fig. 3c) showed m/z 237 corresponding to the loss of 17 Da ($-NH_3$), m/z 212 (loss of

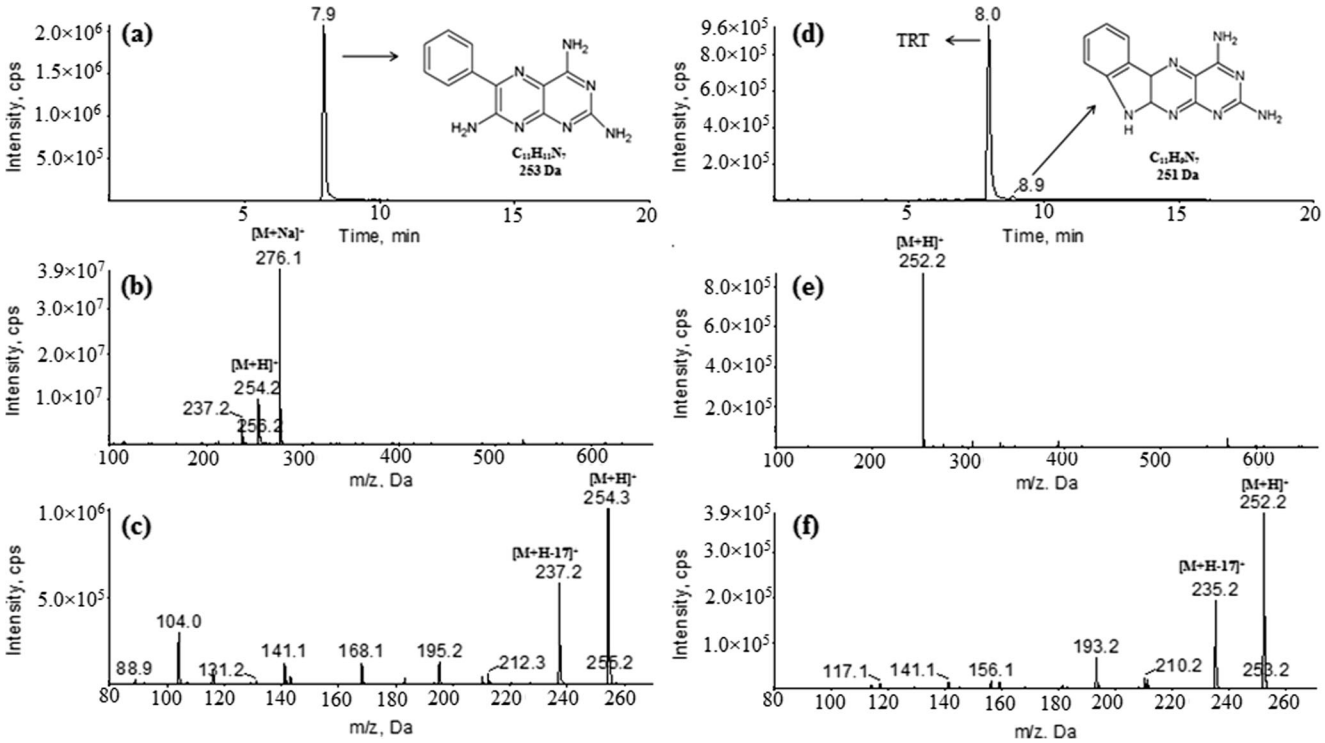

Fig. 3 **a** TIC of control sample. (**b**) Mass spectra of 7.9-min peak detected in (**a**). **c** Fragment ion spectra of m/z 254. **d** TIC of electrolysis sample. **e** Mass spectra of 8.9-min peak detected in (**d**). **f** Fragment ion spectra of m/z 252

Table 2 Parameter, levels, and results of the 2^3 factorial design

Parameter				Minimum (−)	Central Point (0)		Maximum (+)	
f (Hz)				30	55		80	
E_{sw} (mV)				2	6		10	
ΔE (mV)				10	55		100	
Exp.	E_{sw}	ΔE	f	I_{ap} (μA)	*B.L.* (μA)	*di* I_{ap}	*di* B.L.	O.D.
1	+	+	+	116	280	1.000	0.000	0.000
2	−	+	+	39.5	162	0.278	0.435	0.348
3	+	−	+	31.6	44.0	0.204	0.869	0.421
4	−	−	+	20.1	19.8	0.097	0.958	0.305
5	+	+	−	49.5	110	0.372	0.626	0.483
6	−	+	−	14.6	49.0	0.046	0.851	0.197
7	+	−	−	28.0	19.5	0.171	0.959	0.405
8	−	−	−	9.74	8.50	0.000	1.000	0.000
9[a]	0	0	0	50.5	98.0	0.382	0.670	0.506
9[a]	0	0	0	54.2	101	0.416	0.659	0.524
9[a]	0	0	0	52.5	99.0	0.400	0.667	0.517
9[a]	0	0	0	51.9	100	0.395	0.663	0.512
9[a]	0	0	0	50.9	99.0	0.386	0.667	0.507

f frequency, E_{sw} step potential, ΔE pulse amplitude

[a] Replicas of the central point

42 Da, $-NCNH_2$), and *m/z* 195 (loss of 59 Da, $-NH_3$ and $-NCNH_2$); the same losses were observed to the oxidation product as the fragments obtained were *m/z* 235, 210, and 193 (Fig. 3f). The high similarity between both spectra has led to the proposal of the structure found at Fig. 3d.

Electroanalytical determination of TRT

In order to obtain TRT low detection levels besides the use of GECE/MPs-To, the performance of linear scan, differential pulse, and square wave voltammetric techniques were compared. For this, voltammograms were recorded for 100 μmol L^{-1} of TRT in 0.10 mol L^{-1} B–R buffer solution (pH 6.0). The peak current intensity increased almost 44 and 85 % for the square wave voltammetry compared to linear scan voltammetry and differential pulse voltammetry, respectively. Thus, the square wave technique was chosen for the quantification of the diuretic.

The parameters of square wave voltammetry technique were optimized aiming at determining of TRT through the 2^3 factorial design, Doehlert matrix, and multi-response methodology [41–43]. The analytical signals (I_{ap} and base line) from the 2^3 factorial design, designated overall desirability, as well as their parameters and levels are shown in Table 2. Besides the experiments from the 2^3 factorial design, the central point was included in the planning in order to analyze the behavior between the minimum points (−) and maximum (+). To calculate the overall desirability of each experiment, individual desirabilities (*di*) were determined. The individual desirability is expressed as a dimensionless value ranging from 0 (undesired response) to 1 (desired response). Since the objective is to maximize I_{ap}, individual desirability for each experiment can be calculated using the following equation:

$$di_{I_{ap}} = \frac{(y-L)}{(H-L)} \quad (1)$$

where y is the value obtained experimentally, L is the lowest value obtained among all experiments performed, and H is the highest value obtained from all the

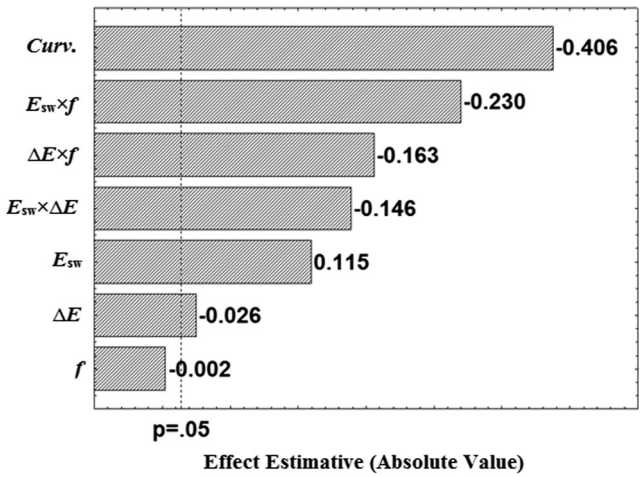

Fig. 4 Pareto diagram of the responses obtained in the 2^3 factorial design

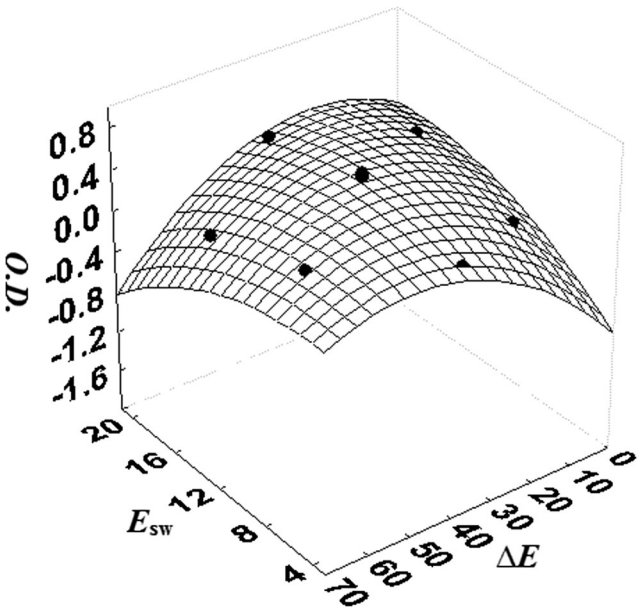

Fig. 5 Response surfaces for $E_{sw} \times \Delta E$

Table 3 Doehlert matrix used for optimizing E_{sw} and ΔE

Exp.	E_{sw} (mV)	ΔE (mV)	I_{pa} (μA)	*B.L.* (μA)	*di* I_{pa}	*di* B.L.	O.D.
1	12 (0)	35 (0)	53.5	52.5	0.593	0.487	0.537
1	12 (0)	35 (0)	50.6	53.0	0.549	0.479	0.513
1	12 (0)	35 (0)	48.5	52.6	0.517	0.485	0.501
1	12 (0)	35 (0)	47.5	52.6	0.502	0.483	0.492
1	12 (0)	35 (0)	46.0	52.7	0.480	0.484	0.482
2	20 (1)	35 (0)	44.4	74.8	0.455	0.181	0.287
3	16 (0.5)	60 (0.866)	80.6	88.2	1.000	0.000	0.000
4	4 (−1)	35 (0)	21.1	29.7	0.106	0.799	0.291
5	8 (−0.5)	10 (−0.866)	14.1	15.0	0.000	1.000	0.000
6	16 (0.5)	10 (−0.866)	19.6	24.4	0.083	0.871	0.268
7	8 (−0.5)	60 (0.866)	35.0	64.0	0.314	0.329	0.322

experiments analyzed. However, to the base line (*B.L.*), the smaller value is a better response; thereby, the calculation of the individual desirability for this response may be made using Eq. 2:

$$di_{\mathrm{B.L.}} = \frac{(H-y)}{(H-L)}. \tag{2}$$

Thus, possession of the individual desirabilities, the overall desirability (O.D.) was determined by the geometric mean of individual desirabilities, as shown in Eq. 3:

$$\mathrm{O.D.} = \sqrt{\left(di_{I_{ap}}\right)\left(di_{\mathrm{B.L.}}\right)}. \tag{3}$$

The responses in O.D. were used for statistical treatment. As shown in Fig. 4, all parameters and interactions presented negative effect except the parameter E_{sw}. This indicates that the best answers are obtained when the parameters ΔE and f are at their lowest levels, while for the parameter E_{sw}, the best answer was observed at their highest level. At the 95 % significance level, the effect of all interactions and parameters was significant except for the parameter f that was not significant for the method.

Among all the results shown in the Pareto diagram, the curvature (Curv.) was the most significant study to the work. The Curv. is given by the following equation [44]:

$$\mathrm{Curv.} = R_{ed} - R_{cp}, \tag{4}$$

where R_{ed} is the average responses obtained from experiments specified by the factorial design and R_{cp} is the average responses obtained for the central point. Thus, a positive value indicates that the best answers are acquired for the points belonging to the factorial design while a negative value for the Curv. indicates that best results are found for the points near the central point. Thus, as shown in Fig. 5, the effect for the Curv. presented a negative result, indicating that the best responses are obtained for values of the center point. Since the parameters E_{sw} and ΔE were significant for the method, a more detailed study was carried by Doehlert matrix. As f showed no significance for the method at level 95 %, the frequency was set at its lowest level (30 Hz), where the best responses were obtained.

For Doehlert matrix, the same analytical responses were used (I_{ap} and B.L.). Thus, the responses were converted in terms of *di* according to Eqs. 1 and 2 and then in O.D.

Table 4 ANOVA for the results obtained of the Doehlert matrix

Factor	Square sum (SS)	Degrees of freedom (d.f.)	Mean square (MS)	$F_{calc.}$
E_{sw}	0.000314	1	0.000314	0.692
E_{sw}^2	0.0667	1	0.0667	147
ΔE	0.000716	1	0.000716	1.58
ΔE^2	0.234	1	0.234	516
$E_{sw} \times \Delta E$	0.0870	1	0.0870	192
lack of fit	0.000410	1	0.000410	0.904
pure error	0.00181	4	0.000454	
Total	0.380	10		

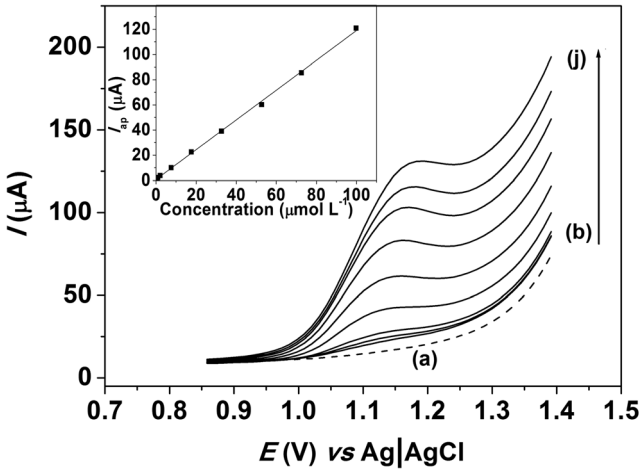

Fig. 6 Square wave voltammograms in 0.10 mol L^{-1} B–R buffer solution (pH 6.0) for supporting electrolyte (*a*) and for the concentrations of 0.500 (*b*), 1.00 (*c*), 2.00 (*d*), 7.60 (*e*), 17.6 (*f*), 32.7 (*g*), 52.7 (*h*), 72.6 (*i*), and 99.8 μmol L^{-1} (*j*) for TRT. Respective analytical curve obtained for I_{ap} vs [TRT] (*insert*). *f*: 30 Hz, ΔE: 36.2 mV, E_{sw}: 11.5 mV

(Eq. 3). The results of Doehlert matrix are shown in Table 3. Through analysis of variance (ANOVA), it was verified that the values of F calculated ($F_{calc.}$) were lower than the value of F tabulated ($F_{tab.}$) for the parameters E_{sw} and ΔE, both linear. This indicates that the levels for the parameters E_{sw} and ΔE were studied in a satisfactory range (Table 4). In addition, the value of $F_{calc.}$ ($MS_{lack\ of\ fit}/MS_{pure\ error}$) was of 0.903 being lower than the value of $F_{tab.}$, that is of 7.71, indicating that the results are suited to the linear quadratic model, having a value of R^2 of 0.994 and R^2 adjusted of 0.988.

Thus, the statistical model obtained from the Doehlert matrix is given by the following equation:

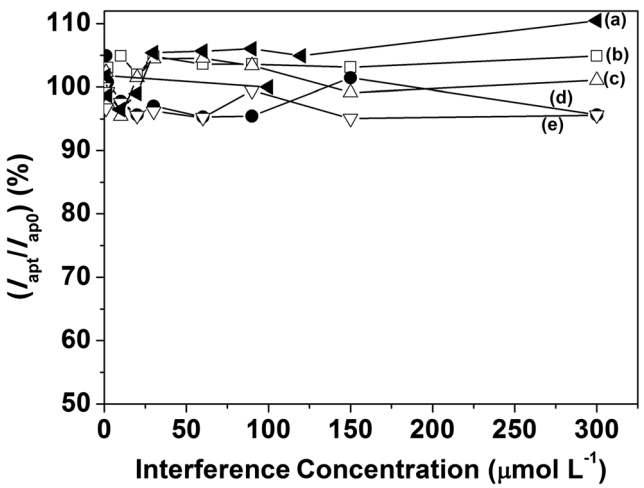

Fig. 7 Effect in the I_{ap} for a concentration of 30.0 μmol L^{-1} of TRT in the presence of some substances in the urine in 0.10 mol L^{-1} B–R buffer solution (pH 6.0). CR (*a*), UA (*b*), UR (*c*), GL (*d*), and AA (*e*)

Table 5 Recoveries of TRT in tap water samples using the GECE/MPs-To electrode

Sample	Sample 1	Sample 2	Sample 3
Added (μmol L^{-1})	15.00	15.00	15.00
Found (μmol L^{-1})	15.50±0.84	14.80±0.96	15.20±0.83
Recoveries (%)	103.00	98.70	102.00
$t_{cal.}$	0.93	0.34	0.45

$t_{crit.}$=4.30; n=3

$$\text{O.D.} = 0.505 - 0.0100 \times E_{sw} - 0.216 \times E_{sw}^2 + 0.0130 \times \Delta E - 0.303 \times \Delta E^2 - 0.295 \times E_{sw} \times \Delta E. \quad (5)$$

Therefore, the statistical model above was derived, so maximum values of E_{sw} (11.5 mV) and ΔE (36.2 mV) were obtained. In Fig. 5, the response surface from the Eq. 5 is shown.

Analytical curve

Figure 6 illustrates the square wave voltammograms obtained for the diuretic TRT from 0.500 to 99.8 μmol L^{-1} in 0.10 mol L^{-1} B–R buffer solution (pH 6.0) under optimized conditions. Good linear relationship was obtained in all concentration presenting the following linear relationship: $I_{ap}=(1.180\pm0.013)\times[TRT]+(0.7\pm0.6)\times10^{-7}$ (R^2=0.999) as shown in the insert of Fig. 6. The limits of detection (L.D.) and quantitation (L.Q.) were calculated using the following equations: L.D. = 3std/*m* and L.Q. = 10std/*m*, where std is the standard deviation of 10 square wave voltammograms only

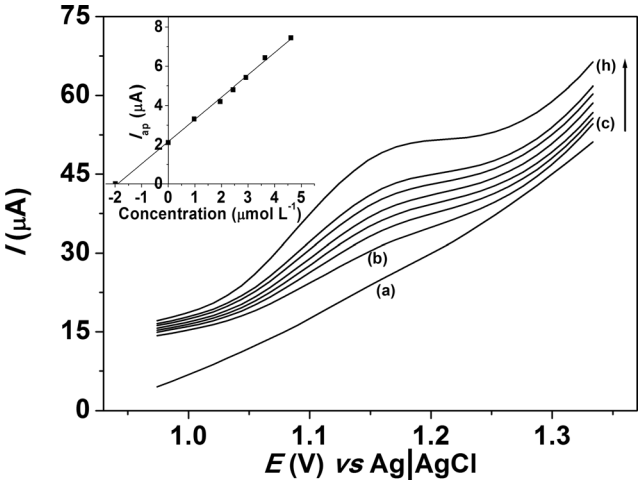

Fig. 8 Square wave voltammograms recorded for 0.10 mol L^{-1} B–R buffer solution (pH 6.0) for supporting electrolyte (*a*), addition of 2 mL of sample (*b*), and successive standard additions of TRT in the concentrations of 0.980 (*c*), 1.95 (*d*), 2.44 (**e**), 2.92 (*f*), 3.64 (*g*), and 4.61 μmol L^{-1} (*h*) using the GECE/MPs-To. Insert: Respective analytical curve obtained for I_{ap} *vs* [TRT]. *f*: 30 Hz, ΔE: 36.2 mV, E_{sw}: 11.5 mV

with the supporting electrolyte (0.100 mol L^{-1} B–R buffer solution pH 6.0) and *m* the slope of the curve. Thus, the values for L.D. and L.Q. were 1.47 and 4.91×10^{-7} mol L^{-1}, respectively.

The repeatability of the method was tested through 10 consecutive analyzes for TRT solution at concentrations of 1.50 and 80.0×10^{-6} mol L^{-1}, where the relative standard deviation was 4.10 and 3.24 %, respectively, indicating that the proposed electrode is not poisoned in consecutive tests since the solution is stirred between measurements.

Interference study

The influence of possible interfering compounds such as uric acid (UA), urea (UR), ascorbic acid (AA), glucose (GL), and creatinine (CR) on the peak currents recoveries of TRT determination as well as on the peak resolution was examined. Under optimized conditions, square wave voltammograms were recorded for a solution containing 30.0 μmol L^{-1} of TRT and the possible interfering in different concentrations comprising the range of 1.00 to 300 μmol L^{-1}. As can be seen in Fig. 7, the percentages between the I_{ap} of the TRT in the presence of interference (I_{apt}) about the I_{ap} of the TRT (I_{ap0}) for substances UA (b), UR (c), GL (d), and AA (e) were in the range of 101–104, 95.0–104, 95.0–104, and 95.0–99.0 %, respectively, verifying that these substances showed no interference in I_{ap} of the TRT in the concentration range studied. However for CR (a), no interference was observed for the concentration range of 1.00 to 120 μmol L^{-1}, where the percentage of I_{apt}/I_{ap0} was between 96.0 and 106 %. Nonetheless, for concentration of 300 mmol L^{-1} of CR, a relationship between I_{apt}/I_{ap0} of 110 % was observed, indicating that in higher concentrations, the CR can act as a possible interference in the determination of TRT diuretic.

Application of the GECE/MPs-To to the analysis of TRT in human urine samples

Firstly, the performance of the proposed sensor was tested in tap water samples to evaluate the method recovery. For this, tap water samples were spiked to 15.0 μmol L^{-1} TRT. The recovery was verified by the standard addition method, where the added and recovered values are shown in Table 5. As can be seen, for all samples, the recoveries were between 98.7 and 103 %. The calculated value of *t* ($t_{calc.}$) was smaller than *t* tabulated ($t_{tab.}$), indicating that there is significant difference at 95 % confidence between the fortified and recovered concentration. In addition, the recoveries of TRT in tap water did not exceed 3.30 % error, indicating good applicability of the method.

Afterwards, the applicability of the GECE/MPs-To to determine TRT in human urine sample was tested. As described in the experimental part (section "Urine samples"), an aliquot of spiked urine with 4.93 μmol L^{-1} of TRT was added in the electrochemical cell without prior treatment of the sample. The respective voltammogram is shown in Fig. 8 before ("a" for supporting electrolyte and "b" for human urine sample) and after (c to h) successive standard additions of TRT. An excellent linear relationship was obtained, and a value of 4.97 ±0.150 μmol L^{-1} was found (Fig. 8, insert), which represent 101 % of recovery.

The method was validated by using LC-MS/MS where the urine sample was treated as previously described in section "Urine samples." The chromatographic peak employed for quantification was observed in the t_r of 3.39 min which corresponds to the most intense transition monitored (first transition showed at Table 1). Beside the analyses of the sample by standard additions, the concentration found by LC-MS/MS technique was 5.20±0.18 μmol L^{-1}, representing 105 % of recovery.

Calculating the Student's *t* test (paired *t* test), a value of 3.83 was found, where the calculated value is less than the value of $t_{crit.}$ (4.30) [45]. Thus, the results for the recovery of the TRT in the human urine sample by the proposed method showed no significant difference at 95 % confidence compared to LC-MS/MS technique.

Conclusion

In this work, a simple and reliable electroanalytical method based on a graphite-epoxy composite electrode modified by tosyl-functionalized magnetic particles (GECE/MPs-To) for determination of the triamterene diuretic in human urine sample was proposed. After multivariate optimization of the inherent parameters of the square wave voltammetry, an analytical curve was constructed in wide linear range and low limit of detection plus excellent repeatability for different concentrations. The GECE/MPs-To was successfully applied in human urine sample where there was no significant difference when compared to LC-MS/MS technique. Finally, this work is an attractive method for environmentally friendly detection.

Acknowledgments The authors gratefully acknowledge the financial support from Fundação de Amparo à Pesquisa do Estado de São Paulo (FAPESP), CAPES, and CNPq.

References

1. Yang J, Park S-B, Yoon H-G, Huh Y-M, Haam S (2006) Preparation of poly ε-caprolactone nanoparticles containing magnetite for magnetic drug carrier. Int J Pharm 324:185–190
2. Hu FX, Neoh KG, Kang ET (2006) Synthesis and in vitro anticancer evaluation of tamoxifen-loaded magnetite/PLLA composite nanoparticles. Biomaterials 27:5725–5733

3. Ma Z, Liu H (2007) Synthesis and surface modification of magnetic particles for application in biotechnology and biomedicine. China Part 5:1–10
4. Luo Y-L, Fan L-H, Xu F, Chen Y-S, Zhang C-H, Wei Q-B (2010) Synthesis and characterization of Fe_3O_4/PPy/P(MAA-co-AAm) trilayered composite microspheres with electric, magnetic and pH response characteristics. Mater Chem Phys 120:590–597
5. Shahbazi F, Amani K (2014) Synthesis, characterization and heterogeneous catalytic activity of diamine-modified silica-coated magnetite-polyoxometalate nanoparticles as a novel magnetically-recoverable nanocatalyst. Catal Commun 55:57–64
6. Shan Z, Li C, Zhang X, Oakes KD, Servos MR, Wu Q, Chen H, Wang X, Huang Q, Zhou Y, Yang W (2011) Temperature-dependent selective purification of plasmid DNA using magnetic nanoparticles in an RNase-free process. Anal Biochem 412:117–119
7. Liu JW, Zhang Y, Chen D, Yang T, Chen ZP, Pan SY, Gu N (2009) Facile synthesis of high-magnetization γ-Fe2O3/alginate/silica microspheres for isolation of plasma DNA. Colloids Surf A: Physicochem Eng Aspects 341:33–39
8. Garcia J, Zhang Y, Taylor H, Cespedes O, Webb ME, Zhou D (2011) Multilayer enzyme-coupled magnetic nanoparticles as efficient reusable biocatalysts and biosensors. Nanoscale 3:3721–3730
9. Kong L, Lu X, Jin E, Jiang S, Bian X, Zhang W, Wang C (2009) Constructing magnetic polyaniline/metal hybrid nanostructures using polyaniline/Fe_3O_4 composite hollow spheres as supports. J Solid State Chem 182:2081–2087
10. Heli H, Majdi S, Sattarahmady N, Parsaei A (2010) Electrocatalytic oxidation and sensitive detection of deferoxamine on nanoparticles of Fe_2O_3@NaCo[Fe(CN)$_6$]-modified paste electrode. J Solid State Electrochem 14:1637–1647
11. Alizadeh T, Jamshidi F (2015) Synthesis of nanosized sulfate-modified α-Fe_2O_3 and its use for the fabrication of all-solid-state carbon paste pH sensor. J Solid State Electrochem 19:1053–1062
12. Hu Y, Zhang Z, Zhang H, Luo L, Yao S (2012) Selective and sensitive molecularly imprinted sol–gel film-based electrochemical sensor combining mercaptoacetic acid-modified PbS nanoparticles with Fe_3O_4@Au–multi-walled carbon nanotubes–chitosan. J Solid State Electrochem 16:857–867
13. Yang S, Li G, Wang G, Deng D, Qu L (2015) A novel electrochemical sensor based on Fe_2O_3 nanoparticles/N-doped graphene for electrocatalytic oxidation of L-cysteine. J Solid State Electrochem. Doi:10.1007/s10008-015-2980-y
14. Pailleret A, Hien NTL, Thanh DTM, Deslouis C (2007) Surface reactivity of polypyrrole/iron-oxide nanoparticles: electrochemical and CS-AFM investigations. J Solid State Electrochemi 11:1013–1021
15. Lermo A, Fabiano S, Hernández S, Galve R, Marco M-P, Alegret S, Pividori MI (2009) Immunoassay for folic acid detection in vitamin-fortified milk based on electrochemical magneto sensors. Biosens Bioelectro 24:2057–2063
16. Mani V, Wu T-Y, Chen S-M (2014) Iron nanoparticles decorated graphene-multiwalled carbon nanotubes nanocomposite-modified glassy carbon electrode for the sensitive determination of nitrite. J Solid State Electrochem 18:1015–1023
17. Petcharoena K, Sirivat A (2012) Synthesis and characterization of magnetite nanoparticles via the chemical co-precipitation method. Mat Sci Eng B 177:421–427
18. Mahdaviana AR, Mirrahimib MA-S (2010) Efficient separation of heavy metal cations by anchoring polyacrylic acid on superparamagnetic magnetite nanoparticles through surface modification. Chem Eng J 159:264–271
19. Una B, Durmus Z, Kavas H, Baykal A, Toprak MS (2010) Synthesis, conductivity and dielectric characterization of salicylic acid–Fe_3O_4 nanocomposite. Mater Chem Phys 123:184–190
20. Liu X, Kaminski MD, Guan Y, Chen H, Liu H, Rosengart AJ (2006) Preparation and characterization of hydrophobic superparamagnetic magnetite gel. J Magn Magn Mater 306:248–253
21. Bruce IJ, Taylor J, Todd M, Davies MJ, Borioni E, Sangregorio C, Sen T (2004) Synthesis, characterisation and application of silica-magnetite nanocomposites. J Magn Magn Mater 284:145–160
22. Asuha S, Suyala B, Siqintana X, Zhao S (2011) Direct synthesis of Fe_3O_4 nanopowder by thermal decomposition of Fe–urea complex and its properties. J Alloy Compd 509:2870–2873
23. Laube T, Kergaravat SV, Fabiano SN, Hernández SR, Alegret S, Pividori MI (2011) Magneto immunosensor for gliadin detection in gluten-free foodstuff: Towards food safety for celiac patients. Biosens Bioelectro 27:46–52
24. Bagheri H, Afkhami A, Panahi Y, Khoshsafar H, Shirzadmehr A (2014) Facile stripping voltammetric determination of haloperidol using a high performance magnetite/carbon nanotube paste electrode in pharmaceutical and biological samples. Mat Sci Eng C 37:264–270
25. Yin H, Zhou Y, Ma Q, Ai S, Chen Q, Zhu L (2010) Electrocatalytic oxidation behavior of guanosine at graphene, chitosan and Fe_3O_4 nanoparticles modified glassy carbon electrode and its determination. Talanta 82:1193–1199
26. Deventer K, Pozo OJ, Eenoo PV, Delbeke FT (2009) Qualitative detection of diuretics and acidic metabolites of other doping agents in human urine by high-performance liquid chromatography–tandem mass spectrometry: Comparison between liquid–liquid extraction and direct injection. J Chromatogr A 1216:5819–5827
27. Goebel C, Trout GJ, Kazlauskas R (2004) Rapid screening method for diuretics in doping control using automated solid phase extraction and liquid chromatography-electrospray tandem mass spectrometry. Anal Chim Acta 502:65–74
28. The World Anti-Doping Code: The 2014 prohibited list (2015). http://list.wadaama.org/wp-content/uploads/2013/11/2014-Prohibited-List-ENGLISH-FINAL.pdf. Accessed 25 Sept 2015
29. Maher HM, Youssef RM, El-Kimary EI, Hassana EM, Barary MA (2012) Bioavailability study of triamterene and xipamide using urinary pharmacokinetic data following single oral dose of each drug or their combination. J Pharmaceut Biomed 61:78–85
30. Tabrizi AB, Naini S, Parnian K, Mohammadi S, Zad FE, Anvarian SP, Abdollahi A (2014) Determination of triamterene in human plasma and urine after its cloud point extraction. Quim Nov. 37:1182–1187
31. Sanchez FG, Diaz AN, Guerrero MML (2015) Time-Resolved Spectroscopy for Selective Determination of Fluorescent Diuretics. Spectrosc Lett 48:481–486
32. Brunelli C, Bicchi C, Stilo AD, Salomone A, Vincenti M (2006) High-speed gas chromatography in doping control:Fast-GC and fast-GC/MS determination ofb-adrenoceptor ligands and diuretics. J Sep Sci 29:2765–2771
33. Nezhadali A, Mojarrab M (2015) Fabrication of an electrochemical molecularly imprinted polymer triamterene sensor based on multivariate optimization using multi-walled carbon nanotubes. J Electroanal Chem 744:85–94
34. Ensafi AA, Hajian R (2008) Determination of Losartan and Triamterene in Pharmaceutical Compounds and Urine Using Cathodic Adsorptive Stripping Voltammetry. Anal Sci 24:1449–1454
35. Merás ID, Mansilla AE, López FS, Gómez MJR (2002) Determination of triamterene and leucovorin in biological fluids by UV derivative-spectrophotometry and partial least-squares (PLS-1) calibration. J Pharmaceut Biomed 27:81–90
36. Lermo A, Zacco E, Barak J, Delwiche M, Campoy S, Barbé J, Alegret S, Pividori MI (2008) Towards Q-PCR of pathogenic bacteria with improved electrochemical double-tagged genosensing detection. Biosens Bioelectro 23:1805–1811
37. Erdem A, Pividori MI, Lermo A, Bonanni A, Valle M, Alegret S (2006) Genomagnetic assay based on label-free electrochemical

detection using magneto-composite electrodes. Sensor Actuat B-Chem 114:591–598
38. Murray GJ, Danaceau JP (2009) Simultaneous extraction and screening of diuretics, beta-blockers, selected stimulants and steroids in human urine by HPLC-MS/MS and UPLC-MS/MS. J Chromatogr B 877:3857–3864
39. Bard AJ, Faulkner LR (2001) Electrochemical methods: fundamentals and applications, 2nd edn. Wiley, New York
40. Sartori ER, Takeda HH, Fatibello-Filho O (2011) Glassy Carbon Electrode Modified with Functionalized Carbon Nanotubes Within a Poly(allylamine hydrochloride) Film for the Voltammetric Determination of Sulfite in Foods. Electroanal 23:2526–2533
41. Neto BB, Scarminio IS, Bruns RE (2010) Como fazer experimentos, fourth edn. Bookman, Brazil
42. Ferreira SLC, Santos WNL, Quintella CM, Neto BB, Bosque-Sendra JM (2004) Doehlert matrix: a chemometric tool for analytical chemistry—review. Talanta 63:1061–1067
43. Hudari FF, Duarte EH, Pereira AC, Dall'Antonia LH, Kubota LT, Tarley CRT (2013) Voltammetric method optimized by multi-response assays for the simultaneous measurements of uric acid and acetaminophen in urine in the presence of surfactant using MWCNT paste electrode. J Electroanal Chem 696:52–58
44. Jesus RM, Silva LOB, Castro JT, Neto ADA, Jesus RM, Ferreira SLC (2013) Determination of mercury in phosphate fertilizers by cold vapor atomic absorption spectrometry. Talanta 106:293–297
45. Miller JC, Miller JN (1988) Statistics for analytical chemistry, 2nd edn. Ellis Horwood Limited, England